



# Hydrothermal synthesis and magnetic properties of Fe<sup>3+</sup>-doped multiferroic hexagonal rare-earth manganates



Li Guo<sup>a</sup>, Zhiqiang Zhou<sup>a,\*</sup>, Hongming Yuan<sup>b</sup>

<sup>a</sup> College of Sciences, Northeast Forestry University, Harbin 150040, PR China

<sup>b</sup> State Key Laboratory of Inorganic Synthesis and Preparative Chemistry, College of Chemistry, Jilin University, Changchun 130012, PR China

## ARTICLE INFO

### Article history:

Received 24 May 2014

Received in revised form 20 July 2014

Accepted 21 July 2014

Available online 30 July 2014

### Keywords:

Hexagonal manganate

Multiferroic

Antiferromagnetic transition

Fe doping

## ABSTRACT

Hexagonal  $\text{RMn}_{1-x}\text{Fe}_x\text{O}_3$  ( $\text{R} = \text{Er, Tm, Yb and Lu}$ ;  $x = 0, 0.1, 0.3$  and  $0.5$ ) were successfully synthesized via the low-temperature hydrothermal technique.  $\text{Fe}^{3+}$  doping was used to elevate the low antiferromagnetic transition temperature  $T_N$  which is a fatal weakness for hexagonal manganates  $\text{RMnO}_3$  to be used as multiferroic materials. The structures, compositions, morphologies and magnetic properties of the samples and the valences of Mn and Fe were studied via the methods of XRD, Rietveld refinement, ICP-MS, EDS, SEM, SQUID and XPS.  $\text{ErMnO}_3$  and  $\text{RMn}_{1-x}\text{Fe}_x\text{O}_3$  ( $\text{R} = \text{Tm, Yb and Lu}$ ;  $x = 0, 0.1, 0.3$  and  $0.5$ ) were all of pure hexagonal structure while  $\text{ErMn}_{1-x}\text{Fe}_x\text{O}_3$  ( $x = 0.1, 0.3$  and  $0.5$ ) comprised hexagonal and orthorhombic structures. As for the undoped  $\text{RMnO}_3$  ( $\text{R} = \text{Er, Tm, Yb and Lu}$ ), the cell parameters  $a$ ,  $c$  and cell volume  $V$  decreased while the antiferromagnetic transition temperatures  $T_N$  rose with the decrease of  $\text{R}^{3+}$  radius. The antiferromagnetic transition temperatures  $T_N$  were elevated by  $\text{Fe}^{3+}$  doping and a linear relation was observed between  $\Delta T_N$  and Fe doping concentration  $x$ . A percentage of  $\text{Fe}^{3+}$  doping elevated  $T_N$  by 0.3–0.5 K, and the elevation was more obvious when the  $\text{R}^{3+}$  ionic radius was smaller.

© 2014 Elsevier B.V. All rights reserved.

## 1. Introduction

The hexagonal rare-earth manganates  $\text{h-RMnO}_3$  ( $\text{R} = \text{Ho, Er, Tm, Yb, Lu, Sc and Y}$ ) are potential candidates for single-phased multiferroic materials integrating ferroelectricity and antiferromagnetism, and so attract great attention in the fields of functional materials and condensed matter physics in recent years [1–7].

The antiferromagnetic (AFM) transition temperatures  $T_N$  of hexagonal rare-earth manganates  $\text{h-RMnO}_3$  ( $\text{R} = \text{Ho, Er, Tm, Yb, Lu, Sc and Y}$ ) are as low as 70–130 K [8–11] while their ferroelectric Curie temperatures are as high as 570–990 K [12–14]. In the closely packed basal plane, the spin of  $\text{Mn}^{3+}$  is in triangulate arrangement with that of its neighbors. In this case, the AFM spin–spin interaction is geometrically frustrated and the long-range magnetic ordering is restrained, therefore, the AFM ordering temperature  $T_N^{\text{in}}$  is low. The ferroelectricity of  $\text{h-RMnO}_3$  originates from the tilting of  $\text{MnO}_5$  polyhedrons and the buckling of  $\text{R}^{3+}$  layers [9]. The ferroelectric ordering occurs in high temperatures while AFM ordering occurs in low temperatures, and so only in low temperatures may  $\text{h-RMnO}_3$  show multiferroic. As we know, for practical application of a multiferroic material, it should possess magnetic

ordering, electric ordering and their coupling around ambient temperatures. Now, elevation of the AFM transition temperatures  $T_N$  of  $\text{h-RMnO}_3$  is urgently needed. And for this purpose, modification by doping is accepted as an important approach. At present, the research on  $\text{h-RMnO}_3$  modification by doping is mainly focused on  $\text{h-YMnO}_3$  [15–25], and the doping concentrations are generally no more than 30 mol% [26–28]. Therefore, there is still a large room for the doping modification research of  $\text{h-RMnO}_3$ . Rare-earth ferrites  $\text{RFeO}_3$  enjoy high AFM transition temperatures. The  $\text{Fe}^{3+}\text{–O–Fe}^{3+}$  super-exchange interaction is so strong that only high temperatures can make it into unordered paramagnetic state. We may expect to elevate the AFM transition temperatures of  $\text{h-RMnO}_3$  by  $\text{Fe}^{3+}$  doping. Concerning the impact of Fe doping on the ferroelectric transition temperatures, literature shows that, Fe doping produces no significant influence on the ferroelectric transitions of single-phased hexagonal  $\text{YMn}_{1-x}\text{Fe}_x\text{O}_3$  [29].

In this work, we synthesized  $\text{h-RMnO}_3$  ( $\text{R} = \text{Er, Tm, Yb and Lu}$ ) via the hydrothermal technique and modified them with B-site  $\text{Fe}^{3+}$  doping to elevate the AFM transition temperatures.

## 2. Experimental

Analytical reagents  $\text{Fe}(\text{NO}_3)_3 \cdot 9\text{H}_2\text{O}$  ( $\geq 98.5\%$ ),  $\text{R}(\text{NO}_3)_3 \cdot 6\text{H}_2\text{O}$  (99.99%) ( $\text{R} = \text{Er, Tm, Yb and Lu}$ ) and  $\text{KOH}$  ( $\geq 85.0\%$ ) were used as starting materials. The salts were made into aqueous solutions to ensure intensive mixing of the starting materials.

\* Corresponding author.

E-mail address: [zhouzq\\_nefu@163.com](mailto:zhouzq_nefu@163.com) (Z. Zhou).

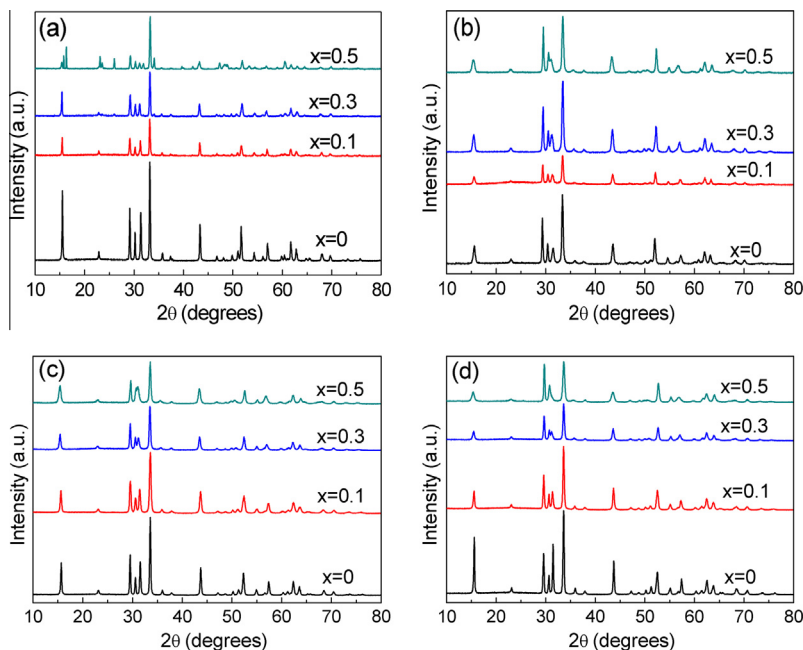


Fig. 1. XRD patterns of the as-prepared  $\text{ErMn}_{1-x}\text{Fe}_x\text{O}_3$  (a),  $\text{TmMn}_{1-x}\text{Fe}_x\text{O}_3$  (b),  $\text{YbMn}_{1-x}\text{Fe}_x\text{O}_3$  (c) and  $\text{LuMn}_{1-x}\text{Fe}_x\text{O}_3$  (d).

Table 1

Cell parameters, cell volumes, atomic occupations and reliability factors of  $\text{h-RMnO}_3$  (R = Er, Tm, Yb and Lu) got from Rietveld refinements.

Compounds	$\text{ErMnO}_3$	$\text{TmMnO}_3$	$\text{YbMnO}_3$	$\text{LuMnO}_3$
<i>Hexagonal (<math>P6_3cm</math>)</i>				
$a$ (Å)	6.1199(0)	6.0840(0)	6.0419(0)	6.0321(0)
$c$ (Å)	11.3949(0)	11.3632(1)	11.3280(0)	11.3577(0)
$V$ (Å <sup>3</sup> )	369.60(2)	364.26(2)	358.12(3)	357.89(2)
R1 2a (0,0,z)				
$z$	0.2721(1)	0.2779(0)	0.2734(5)	0.2705(2)
R2 4a(1/3,2/3,z)				
$z$	0.2313(1)	0.2357(2)	0.2306(3)	0.2266(1)
Mn 6c (x,0,0)				
$x$	0.3399(1)	0.3430(1)	0.3339(1)	0.3212(1)
O1 6c (x,0,z)				
$x$	0.3102(2)	0.2984(2)	0.3035(2)	0.3071(1)
$z$	0.1622(2)	0.1514(1)	0.1706(6)	0.1699(2)
O2 6c (x,0,z)				
$x$	0.6402(3)	0.6422(2)	0.6390(1)	0.6328(2)
$z$	0.3351(4)	0.3241(1)	0.3342(2)	0.3397(2)
O3 2a (0,0,z)				
$z$	0.4812(0)	0.4880(2)	0.4755(1)	0.4836(2)
O4 4b(1/3,2/3,z)				
$z$	0.0161(1)	0.0250(2)	0.0202(1)	0.0189(3)
$R_{wp}$	6.76	8.97	8.85	8.66
$R_p$	5.13	6.35	6.23	6.12

KOH pellets were employed as a mineralizer. As an example, the typical synthesis route of  $\text{TmMn}_{0.5}\text{Fe}_{0.5}\text{O}_3$  was as follows: 10.00 mL  $\text{Tm}(\text{NO}_3)_3$  (0.40 M), 5.00 mL  $\text{Fe}(\text{NO}_3)_3$  (0.40 M) and 3.33 mL  $\text{KMnO}_4$  (0.12 M) were mixed at room temperature, and then KOH pellets were gradually added into the mixture under strong stirring to reach a concentration of 20 M (molar number of KOH/initial solution volume). After the above mixture cooled to room temperature, 2.86 mL  $\text{MnCl}_2$  (0.56 M) was quickly added under stirring. The final mixture was transferred into a Teflon-lined stainless steel autoclave with a filling degree of about 80% to complete crystallization and growth under autogenous pressure at 240 °C for 48 h. After naturally cooled to room temperature, the autoclave was opened and the solid compounds were collected by ultrasonic separation and filtration. The powder was thoroughly washed with deionized water and dried in air at 60 °C to present the final sample.

Powder X-ray diffraction (XRD) was done on a Rigaku D/Max 2500 V/PC X-ray diffractometer with  $\text{Cu K}\alpha$  radiation ( $\lambda = 1.5418$  Å) at 50 kV and 200 mA at room temperature by step scanning in the angle range  $20^\circ \leq 2\theta \leq 80^\circ$  with increments

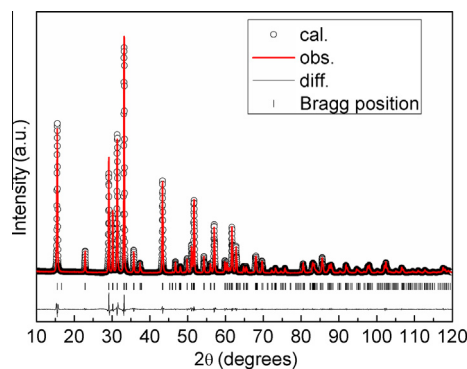


Fig. 2. XRD pattern and Rietveld refinement of  $\text{ErMnO}_3$ .

of 0.02°. Rietveld refinement was performed with Accelrys MS Modeling 4.0. The morphologies were observed with a JEOL JSM-6700F scanning electron microscope (SEM) operated at 5 kV. The chemical compositions were analyzed via Energy Dispersive Spectrometer (EDS) and Inductively Coupled Plasma Mass Spectrometry (ICP-MS) (ICPMS7700, Agilent). The valences were analyzed via X-ray photoelectron spectroscopy (XPS) (PHI-5000 Versaprobe, ULVCA-PHI). The zero-field-cooled (ZFC) and field-cooled (FC) curves were recorded in an applied field of 100 Oe at 2–350 K by Quantum Design MPMS-XL (SQUID).

### 3. Results and discussion

Fig. 1 shows the XRD patterns of the as-prepared  $\text{RMn}_{1-x}\text{Fe}_x\text{O}_3$  (R = Er, Tm, Yb and Lu;  $x = 0, 0.1, 0.3$  and  $0.5$ ). It can be found that,  $\text{ErMn}_{1-x}\text{Fe}_x\text{O}_3$  ( $x = 0.1, 0.3$  and  $0.5$ ) were mixtures of hexagonal and orthorhombic phases;  $\text{ErMn}_{1-x}\text{Fe}_x\text{O}_3$  ( $x = 0$ ),  $\text{TmMn}_{1-x}\text{Fe}_x\text{O}_3$  ( $x = 0, 0.1, 0.3$  and  $0.5$ ),  $\text{YbMn}_{1-x}\text{Fe}_x\text{O}_3$  ( $x = 0, 0.1, 0.3$  and  $0.5$ ) and  $\text{LuMn}_{1-x}\text{Fe}_x\text{O}_3$  ( $x = 0, 0.1, 0.3$  and  $0.5$ ) were all of single hexagonal phase, and no detectable impurity phases were observed.

On the basis of thermodynamic free energy calculation, Graboy et al. [30] pointed out that, with the increase of atomic number (the decrease of ionic radius) of rare earth element (R), the orthorhombic structure of manganates  $\text{RMnO}_3$  gradually becomes unstable while the hexagonal structure becomes stable.  $\text{Er}^{3+}$  is just

Download English Version:

<https://daneshyari.com/en/article/8001036>

Download Persian Version:

<https://daneshyari.com/article/8001036>

[Daneshyari.com](https://daneshyari.com)